

Novel Irreversible Epidermal Growth Factor Receptor Inhibitors by Chemical Modulation of the Cysteine-Trap Portion

Caterina Carmi,[†] Andrea Cavazzoni,[‡] Stefano Vezzosi,[†] Fabrizio Bordi,[†] Federica Vacondio,[†] Claudia Silva,[†] Silvia Rivara,[†] Alessio Lodola,^{*,†} Roberta R. Alfieri,[‡] Silvia La Monica,[‡] Maricla Galetti,[‡] Andrea Ardizzoni,[§] Pier Giorgio Petronini,[‡] and Marco Mor[†]

[†]Dipartimento Farmaceutico, Università degli Studi di Parma, V.le G.P. Usberti 27/A, I-43124 Parma, Italy,

[‡]Dipartimento di Medicina Sperimentale, Università degli Studi di Parma, Via Volturno 39, I-43125 Parma, Italy, and

[§]Oncologia Medica, Azienda Ospedaliero—Universitaria di Parma, V.le Gramsci 14, I-43126 Parma, Italy

Received October 21, 2009

Irreversible EGFR inhibitors can circumvent acquired resistance to first-generation reversible, ATP-competitive inhibitors in the treatment of non-small-cell lung cancer. They contain both a driver group, which assures target recognition, and a warhead, generally an acrylamide or propargylamide fragment that binds covalently to Cys797 within the kinase domain of EGFR. We performed a systematic exploration of the role for the warhead group, introducing different cysteine-trapping fragments at position 6 of a traditional 4-anilinoquinazoline scaffold. We found that different reactive groups, including epoxyamides (compounds 3–6) and phenoxyacetamides (compounds 7–9), were able to irreversibly inhibit EGFR. In particular, at significant lower concentrations than gefitinib (1), (2*R*,3*R*)-*N*-(4-(3-bromoanilino)quinazolin-6-yl)-3-(piperidin-1-ylmethyl)oxirane-2-carboxamide (6) inhibited EGFR autophosphorylation and downstream signaling pathways, suppressed proliferation, and induced apoptosis in gefitinib-resistant NSCLC H1975 cells, harboring the T790M mutation in EGFR.

Introduction

The epidermal growth factor receptor (EGFR^a) is a validated target in cancer treatment strategies. EGFR is a member of the erbB receptor family (erbB1/EGFR, erbB2/HER2, erbB3/HER3, and erbB4/HER4) of tyrosine kinase (TK) that is overexpressed in several human solid tumors and is often associated with more aggressive disease and poorer clinical outcome.^{1,2} Inhibition of the erbB-family receptor tyrosine kinases represented a major advance in the treatment of solid tumors, as demonstrated by the promising clinical activity of the EGFR tyrosine kinase inhibitors 1³ (gefitinib, Figure 1) and *N*-4-(3-ethynylanilino)-6,7-bis(2-methoxyethoxy)quinazoline⁴ (erlotinib, Figure 1). These 4-anilinoquinazoline tyrosine kinase inhibitors compete with ATP in a reversible manner, binding to the kinase domain of the target. Although these drugs have been extremely effective in specific patient populations with tumor-containing mutated oncogenic forms of tyrosine kinases,⁵ the accumulating clinical experience on non-small-cell lung cancers (NSCLCs) indicates that most patients develop resistance.⁶ In approximately half of NSCLC cases that showed an initial response to reversible

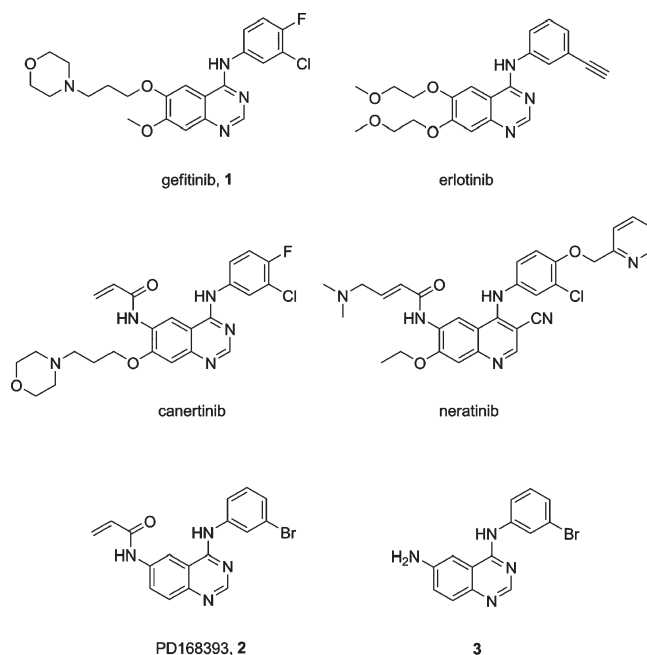
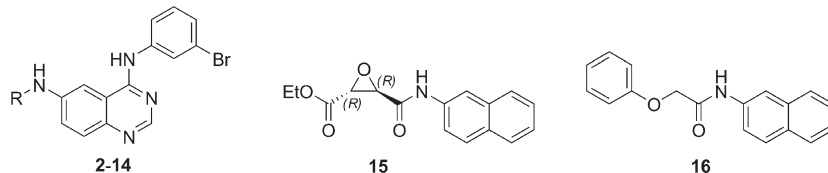


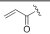
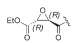
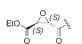
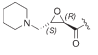
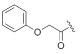
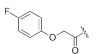
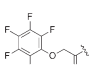
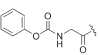
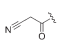
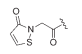
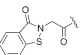
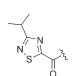
Figure 1. Chemical structures of reversible and irreversible EGFR inhibitors.

EGFR tyrosine kinase inhibitors and subsequently progressed, resistance was associated with the emergence of a secondary mutation within the EGFR kinase domain: substitution of threonine 790 with methionine (T790M).^{6–8} Threonine 790 is the gatekeeper residue in EGFR; its key

*To whom correspondence should be addressed. Phone: +39 0521 905062. Fax: +39 0521 905006. E-mail: alessio.lodola@unipr.it.

^aAbbreviations: EGFR, epidermal growth factor receptor; erbB2, human epidermal growth factor receptor 2; TK, tyrosine kinase; NSCLC, non-small-cell lung cancer; IGF-1R, insulin-like growth factor 1 receptor; PI3K, phosphoinositide-3 kinase; mTOR, mammalian target of rapamycin; MAPK, mitogen activated protein kinase; GSH, glutathione; MTT, 3-(4,5-dimethylthiazol-2-yl)-2,5-diphenyltetrazolium bromide; HBTU, *O*-(benzotriazol-1-yl)-*N,N,N',N'*-tetramethyluronium hexafluorophosphate; DCC, *N,N'*-dicyclohexylcarbodiimide; rmsd, root-mean-square deviation.

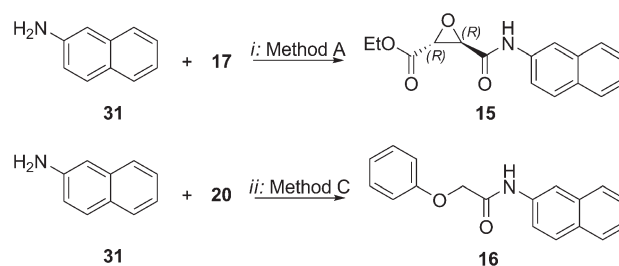
Table 1. EGFR Tyrosine Kinase and Autophosphorylation Inhibition in A431 Cells


Compd	R	kinase assay ^a	autophosphorylation assay ^b			
		IC ₅₀ (nM)	% inhibition (1 μM)		IC ₅₀ (μM)	
			1 h	8 h	1 h	8 h
2		1.69 ± 0.16	98.6 ± 1.4	93.6 ± 6.3	0.012 ± 0.004	0.152 ± 0.037
3	H	n.d.	98.5 ± 1.5	0.0 ± 0.1	0.030 ± 0.010	>10.00
4		0.50 ± 0.12	100.0 ± 0.0	96.6 ± 1.1	0.011 ± 0.007	0.145 ± 0.030
5		0.49 ± 0.04	96.7 ± 3.3	95.7 ± 1.3	0.034 ± 0.009	0.068 ± 0.009
6		1.24 ± 0.13	99.4 ± 0.6	96.3 ± 1.5	0.007 ± 0.001	0.044 ± 0.010
7		9.25 ± 0.71	93.5 ± 7.5	71.4 ± 7.2	0.076 ± 0.054	0.292 ± 0.068
8		8.43 ± 0.16	97.4 ± 1.8	77.6 ± 10.1	0.031 ± 0.008	0.291 ± 0.011
9		23.6 ± 1.75	91.5 ± 4.3	91.4 ± 7.6	0.084 ± 0.037	0.078 ± 0.032
10		0.37 ± 0.05	95.2 ± 0.2	79.9 ± 16.4	n.d.	n.d.
11		0.17 ± 0.02	95.0 ± 3.2	23.6 ± 9.6	n.d.	n.d.
12		0.36 ± 0.08	79.6 ± 8.1	24.7 ± 14.7	n.d.	n.d.
13		0.85 ± 0.05	69.0 ± 16.3	30.7 ± 14.3	n.d.	n.d.
14		129 ± 17.3	82.3 ± 9.1	66.9 ± 13.8	n.d.	n.d.
15		n.d.	0.0 ± 0.1	0.0 ± 0.1	n.d.	n.d.
16		n.d.	0.0 ± 0.1	0.0 ± 0.1	n.d.	n.d.

^a Concentration that inhibits by 50% EGFR tyrosine kinase activity. IC₅₀ values were measured by the phosphorylation of a peptide substrate using time-resolved fluorometry (see Experimental Section). Mean values of three independent experiments ± SEM are reported. ^b Inhibition of EGFR autophosphorylation was measured in A431 intact cells by Western blot analysis. Percent inhibition at 1 μM and IC₅₀ values were measured immediately after and 8 h after removal of the compound from the medium (1 h of incubation). Mean values of at least two independent experiments ± SEM are reported.

group (phoxymethylamides **7**, **8**, and **9**); (iii) carbamoylation (carbamate **10**); (iv) Pinner reaction with formation of a thioimidate adduct (nitrile **11**); (v) disulfide bond formation (isothiazolinone **12**, benzisothiazolinone **13**, and thiadiazole **14**). The covalent interactions could be reversible or irreversible, depending on the reaction products and conditions. Moreover, warhead reactivity was also tentatively modulated by the introduction of electron-withdrawing groups (**7** vs **8** and **9**). In order to test nonspecific toxicity of the considered warheads, we synthesized compounds **15** and **16** (Scheme 2 and Table 1) where two of the cysteine-trap portions within the series were linked to a naphthalene nucleus not able to recognize the molecular target because it is lacking the structural elements required for interaction with the ATP-binding site of EGFR.

The new compounds were tested as EGFR tyrosine kinase inhibitors in enzyme-based and cell-based assays. Effects

Scheme 2. Synthesis of Compounds **15** and **16**^a

^a (i) Method A: dichloromethylene dimethyliminium chloride, NaHCO₃, CH₂Cl₂, 0 °C. (ii) Method C: PCl₅, CH₂Cl₂, reflux.

on downstream signaling pathways and antiproliferative and proapoptotic activities were also investigated in the

gefitinib-resistant H1975 NSCLC cell line harboring the T790M mutation. Structure–activity relationships within the series of synthesized compounds were evaluated in order to identify new irreversible EGFR inhibitors active on a mutated gefitinib-resistant cell line.

Chemistry

The amides (**4–16**) of Table 1 were synthesized by coupling their precursor amines (**3** or **31**) with the appropriate carboxylic acid (**17**, **18**, **20–26**), carboxylate (**19**), or carboxylic ester (**27**), as described in Schemes 1 and 2. 6-Amino-4-(3-bromoanilino)quinazolinone **3** was prepared in three steps from 4-nitroanthranilonitrile **28** as previously described (Scheme 1).^{35,36} Briefly, **28** was refluxed in formic acid and sulfuric acid to give 6-nitro-4-oxoquinazolinone **29**, which was chlorinated with thionyl chloride in dioxane and subsequently treated with 3-bromoaniline to yield 6-nitro-4-(3-bromoanilino)quinazolinone **30**. Reduction of the 6-nitro group with iron and acetic acid in aqueous ethanol gave the 6-amino-4-(3-bromoanilino)quinazolinone **3**.

The epoxy derivatives **4** and **5** were synthesized by coupling **3** with carboxylic acids **17** and **18**, respectively, using dichloromethylene dimethyliminium chloride as the coupling reagent (method A, Scheme 1), while **6** was obtained from **19** with *O*-(benzotriazol-1-yl)-*N,N,N',N'*-tetramethyluronium hexafluorophosphate (HBTU) (method B, Scheme 1). Compounds **7–9** and **11** were prepared as described in method C (Scheme 1) from the amine **3** and the acyl chlorides obtained from **20** (for **7**), **21** (for **8**), **22** (for **9**), or **24** (for **11**). Derivatives **10**, **12**, and **13** were synthesized employing *N,N'*-dicyclohexylcarbodiimide (DCC) as the coupling reagent and **23**, **25**, and **26**, respectively, as carboxylic acids (method D). Finally, amide **14** was obtained by adding potassium *tert*-butoxide to a premixed mixture of ester **27** and amine **3** and exposing the reaction mixture to microwave irradiation (method E, Scheme 1). Amides **15** and **16** were synthesized by reacting 2-naphthylamine **31** with carboxylic acids **17** (method A) and **20** (method C), respectively (Scheme 2).

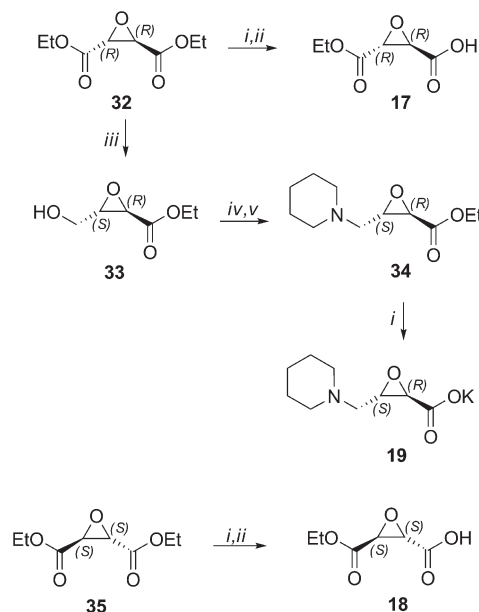
Carboxylic acids **20–24** are commercially available, while **17–19**, **25**, **26**, and the ester **27** were prepared as shown in Schemes 3 and 4. The (2*R*,3*R*)-epoxy diester **32**³⁷ was partially hydrolyzed to the desired (2*R*,3*R*)-monoethyl ester **17**³⁸ or selectively monoreduced to the hydroxyl ester **33**.³⁹ Mesylation of the alcohol **33** and substitution with piperidine gave the epoxy ester **34**, which was hydrolyzed to afford the desired carboxylate **19**. The (2*S*,3*S*)-monoethyl ester **18** was synthesized by partial hydrolysis of the proper (2*S*,3*S*)-epoxy diethyl ester **35**.⁴⁰

The isothiazolinone derivative **25** was synthesized as shown in Scheme 4. 3,3'-Dithiodipropionamide **36**⁴¹ was cyclized with sulfuryl chloride to isothiazolinone **37**,⁴² which was hydrolyzed to the desired carboxylic acid **25** by refluxing in 1 M trifluoroacetic acid. The benzisothiazolinone carboxylic acid **26** and the ethyl 3-isopropyl-1,2,4-thiadiazole-5-carboxylate **27** were prepared as described in Scheme 4, according to literature methods.^{43,44}

Molecular Modeling

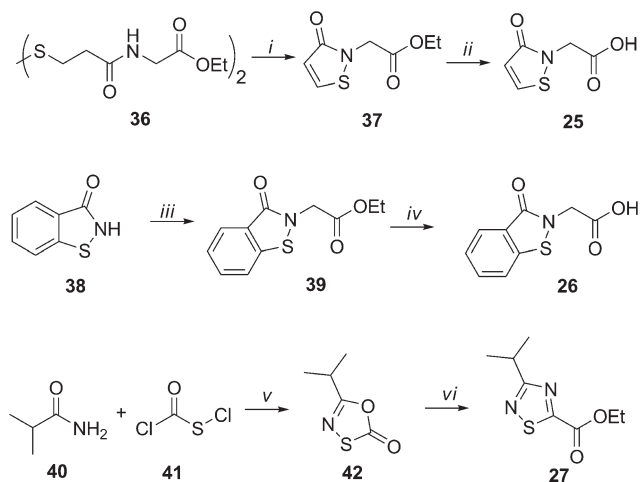
When irreversible enzyme inhibition is required, both warhead reactivity and compound specificity, conferred by a driver portion responsible for noncovalent recognition at the binding site, are important in the search for an effective inhibitor. Cocrystallization of **2** within the catalytic site of

Scheme 3. Synthesis of Warheads **17–19**^a



^a (i) KOH, abs EtOH, 0 °C; (ii) 5% KHSO₄, room temp; (iii) NaBH₄, EtOH, 0 °C; (iv) MsCl, Et₃N, CH₂Cl₂, 0 °C to room temp; (v) anhydrous piperidine, KI, DMF, 0 °C to room temp.

Scheme 4. Synthesis of Warheads **25–27**^a



^a (i) SO₂Cl₂, ClCH₂CH₂Cl, room temp; (ii) 1 M TFA, reflux; (iii) BrCH₂COOEt, Et₃N, THF, room temp; (iv) HCl reflux; (v) CH₂Cl₂, reflux; (vi) NCCOOEt, *p*-xylene, reflux.

EGFR⁴⁵ revealed that this inhibitor covalently binds the Cys797 sulfur atom, adopting an orientation similar to that found for several kinases in complexes with reversible quinazoline inhibitors.⁴⁶ To find out whether the introduction of a warhead differing from the acrylamide chemotype at the quinazolinone ring was consistent with the recognition of the EGFR active site, docking simulations of compounds **4–14** were performed using the publicly available coordinate of the EGFR–2 covalent adduct.⁴⁵ Docking runs revealed that all the inhibitors could be accommodated within EGFR active site with a binding mode resembling that of the acrylamide derivative **2** (Figure 2 and Figure S1–S11, Supporting Information), indicating that the presence of a bulky warhead directly attached, or spaced by an appropriate linker, did not affect the crystallographic-like binding mode of the

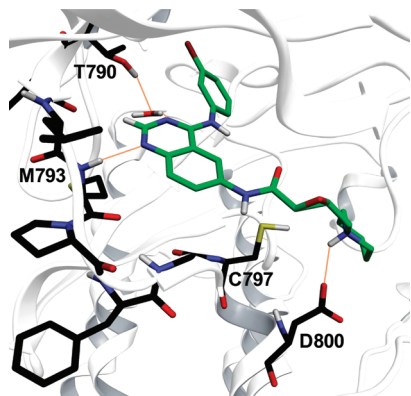


Figure 2. Docking of compound **6** within the EGFR kinase domain. Compound **6** (green carbons) undertakes several polar interactions (highlighted with orange lines) at the EGFR kinase active site (black carbons and white cartoons): (i) a direct hydrogen bond between the quinazoline N1 and the backbone NH of Met793; (ii) a water molecule mediated hydrogen bond between quinazoline N3 and the side chain of Thr790; (iii) a salt bridge between Asp800 and the piperidine nitrogen. The SH group of Cys797 is at 4.13 Å from the closest carbon atom of the epoxy warhead, ready for the nucleophilic attack.

quinazoline moiety.^{23,47–49} Indeed, the two crucial hydrogen bonds between the 4-(3-bromoanilino)quinazoline driving portion and the EGFR active site, one with Met793 and the other, through a conserved water molecule, with Thr790, were formed by all the compounds within the series.

Docking studies also gave information on the positions of the warheads of the new inhibitors with respect to Cys797. Reference compound **2**, docked in its noncovalent form, placed the β -carbon atom of the acrylamide portion at 4.15 Å from the sulfhydryl group of Cys797. Equally, compounds **4–14** placed the reactive center of the warhead at similar distances from this nucleophile (Table S2, Supporting Information). Although the formation of a covalent adduct can be significantly affected by dynamical effects (e.g., trajectory of the nucleophile on the electrophilic center), these docking simulations qualitatively suggested that the warheads of **4–14** may potentially undergo to a nucleophilic attack by Cys797.

Results and Discussion

The newly synthesized 4-(3-bromoanilino)quinazoline derivatives were tested as EGFR inhibitors in enzyme-based and cell-based assays. The effects of the compounds on the kinase activity of human EGFR were quantified by measuring the phosphorylation of a peptide substrate, using time-resolved fluorometry (see Experimental Section). Results are reported in Table 1. In accordance with our docking hypothesis and with the SAR profile of the 4-anilinoquinazoline ring,^{23,47–49} the ATP-binding site of EGFR was tolerant to the introduction of differently sized and shaped substituents at position 6. In the tested conditions, the reference compound **2** showed an IC_{50} of 1.7 nM. Substitution of the acrylamide warhead of **2** with an epoxy (**4–6**), a carbonylic (carbamate **10** and nitrile **11**), or a (benzo)isothiazolinonic (**12** and **13**) one generally produced equally potent or more potent inhibitors. On the contrary, the phenoxyacetamide derivatives (**7–9**) proved less effective than **2** but yet maintained IC_{50} values in the low nanomolar range. Only the introduction of a thiadiazole warhead (**14**) notably reduced EGFR tyrosine kinase inhibition potency.

The ability of the compounds to irreversibly inhibit EGFR autophosphorylation was investigated in the A431 human

epidermoid cancer cell line by Western blotting. Percent inhibitions at 1 μ M are also reported in Table 1. Results were compared with those observed for the reference compounds **2** and **3**, recognized irreversible and reversible EGFR inhibitors, respectively. A431 cells, which overexpress wild type EGFR, were treated with each inhibitor for 1 h and then washed free of drug. The degree of EGFR autophosphorylation was measured either immediately after or 8 h after removal of the inhibitor from the medium.¹⁵ For compounds that showed the highest inhibitory potencies toward EGFR at 1 μ M, dose dependency was investigated and IC_{50} determined (Figure 3 and Table 1). As previously reported,³⁴ compounds showing 80% or greater EGFR inhibition 8 h after their removal from the medium were designated as irreversible inhibitors while compounds showing 20–80% inhibition were designated as partially irreversible ones. Table 1 indicates that reference compound **2** and several of the newly synthesized derivatives, **4–6** and **9**, irreversibly inhibit EGFR activity, with inhibition values higher than 90% after an 8 h washout. On the other hand, compounds **7–8** and **10–14** were only partially irreversible under the tested conditions, with percent inhibition of EGFR autophosphorylation between 24% and 80%. As expected, the reference reversible compound **3**, which completely inhibited EGFR activity after 1 h of treatment at 1 μ M, did not show any inhibitory activity 8 h after its removal from the medium.

Compounds **4–6**, which contain an epoxy group at position 6, irreversibly inhibited EGFR at 1 μ M. In fact, their inhibitory effect persisted up to 8 h after removal from the medium, probably because this class of compounds can undergo nucleophilic attack on the epoxide by Cys797 to generate an enzyme-bond addition product. This mechanism of irreversible action through the alkylation of the Cys797 has been reported in the literature for other warheads.^{23,34} Compounds **4–6** showed dose-dependent inhibition of EGFR autophosphorylation in A431 cells with IC_{50} values comparable to that of **2**. In particular, the (2*R*,3*R*)-ethyl 3-(4-(3-bromoanilino)quinazolin-6-ylcarbonyl)oxirane-2-carboxylate (**4**) had an IC_{50} of 0.011 μ M immediately after 1 h of treatment and an IC_{50} of 0.145 μ M 8 h after the removal of the compound from the reaction medium (Figure 3C and Table 1). Its (2*S*,3*S*)-enantiomer **5** was slightly less potent in inhibiting EGFR after 1 h of treatment (IC_{50} = 0.034 μ M) and showed slightly higher potency 8 h after removal of the compound (IC_{50} = 0.068 μ M, Figure 3D and Table 1). While these limited differences may not accurately establish structure–activity relationships, we surmised that the IC_{50} at 1 h, together with the IC_{50} measured on the purified enzyme, reflects both reversible binding to the EGFR catalytic site, by weak interactions at the enzyme surface, and irreversible binding, due to the formation of a covalent bond with an exposed cysteine. On the other hand, the IC_{50} measured 8 h after ligand removal would stem from the extent of irreversible covalent bonding. As observed for both acrylamide and propargylamide derivatives,^{22,50} the introduction of a basic group in the warhead-containing side chain improved inhibitor potency. The amino group can act as (i) an intramolecular catalyst for nucleophilic additions to the cysteine-reactive center, (ii) a water-solubilizing group, since it points out of the ATP-binding pocket toward the solvent environment, and (iii) an additional site for hydrogen bond recognition with acidic residues within the EGFR binding site. Although docking of compound **6** within the EGFR active site suggests a specific role for its piperidine fragment in ligand recognition,

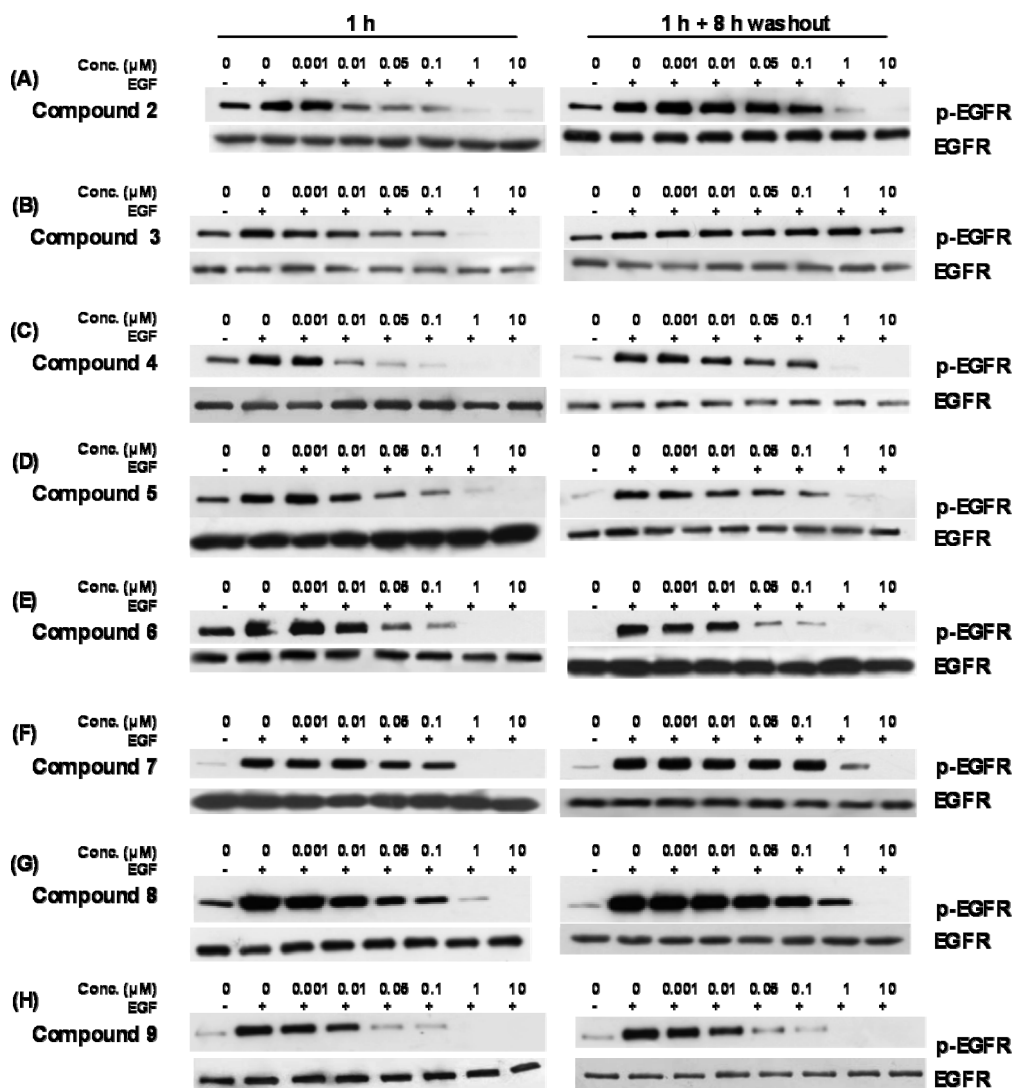


Figure 3. Irreversible inhibitory action of compounds 4–9 on EGFR autophosphorylation. A431 cells were incubated with the investigated compound for 1 h and stimulated with EGF either immediately after or 8 h after removal of the compound from the medium. Western blot analysis was done using monoclonal antibodies directed to p-Tyr1068. **2** and **3** were used as irreversible and reversible reference compounds, respectively. Representative blots of three independent experiments are shown. Total EGFR is shown as loading control.

the presence of the piperidino group does not improve the affinity toward purified EGFR enzyme with respect to the epoxy succinate **4**.

On the other hand, the introduction of a piperidino group increased the inhibitory activity of compound **6** with IC_{50} of 0.007 and 0.044 μM at 1 and 8 h after treatment, respectively (Figure 3E and Table 1). The binding pose, reported in Figure 2, shows that while the 4-anilinoquinazoline portion forms the conventional pattern of hydrogen bonds with the EGFR hinge region,^{13,45,46,51} the protonated nitrogen of the piperidine ring can form an additional hydrogen bond with the acidic group of Asp800.^{52,53} This interaction, rather than improving the recognition of **6** at the active site, may facilitate the nucleophilic attack at the epoxy ring by Cys797.²²

The 6-phenoxyacetamide derivatives **7–9** are potentially able to undergo a nucleophilic attack by Cys797 on their α -methylene, with formation of a covalent adduct with the enzyme and in situ release of a phenol leaving group. Similar chemical approaches to EGFR inhibition have been tried with the α -chloro- and α -methoxyacetamides,²⁴ showing that only the more reactive α -chloroacetamide derivatives give irreversible EGFR inhibition. We introduced the phenoxyacetamide

fragment in view of its intermediate reactivity toward nucleophilic substitutions, which can be further modulated by ring substitution. Compounds **7–9** showed percent inhibitions at 1 μM between 92% and 97%, 1 h after treatment, and between 71% and 91%, 8 h after removal of the compound from the medium. Complete dose–inhibition curves showed that the introduction of a fluorine on the phenoxy aromatic ring did not significantly affect the inhibitory effect of **8** (IC_{50} of 0.076 and 0.292 μM at 1 and 8 h after treatment, respectively) with respect to the unsubstituted **7** (IC_{50} of 0.031 and 0.291 μM). Moreover, the pentafluoro substitution (compound **9**), while it gave a comparable IC_{50} at 1 h after treatment, significantly increased EGFR inhibition after 8 h ($IC_{50} = 0.078 \mu\text{M}$, lower than the reference compound **2**, Figure 3H and Table 1). Since the introduction of the electron-withdrawing fluorine is responsible for increased reactivity toward nucleophilic substitution, the remarkable potency of the pentafluoro substituted derivative **9** under these conditions can be attributed to its increased reactivity versus the nucleophilic Cys797, giving the substitution product. These results indicate that this class shows promise for chemical optimization by modification of the stereoelectronic features of the phenolic leaving group.

Beyond its interest as a warhead, phenoxyacetamide derivatives could also be exploited to design and optimize leaving groups that may be pharmacologically active in a multitarget approach.^{54,55}

Compound **10**, characterized by a carbamate group linked to the quinazoline driver portion through a glycine spacer, gave EGFR inhibition of 95% and 80% at 1 μ M at 1 and 8 h after removal from the medium, respectively. Carbamates can form covalent adducts by carbamylation of serine or cysteine residues, which can be slowly hydrolyzed to re-establish the enzyme in the active form.²⁹ Although EGFR average inhibition at 8 h was less than 90%, this group appeared to be worthy of consideration as a warhead or at least as a starting point for further chemical optimization.

The cyanoacetamide derivative **11** inhibited EGFR autophosphorylation 1 h after treatment at 1 μ M (95% inhibition), while only a residual effect persisted 8 h after washout (24% inhibition). Nitriles are known to form, through a Pinner-like reaction, covalent reversible thioimide ester adducts with biological nucleophiles such as cysteine.²⁹ Compounds **10** and **11** both contain warheads able to establish covalent, reversible interactions with nucleophilic cysteine residues. On the other hand, even though irreversible inhibition was achieved by carbamate derivative **10**, only a residual effect was observed 8 h after treatment with compound **11**, suggesting that the thiocarbamate adduct is more stable than the thioimide ester one. Therefore, although irreversible inhibition might be attained by chemical optimization with this class of derivatives, the nitrile warhead looks less promising than the previously cited ones, with respect to the present target.

Finally, derivatives **12–14** can covalently react with Cys797 via disulfide bond formation, following ring-opening by breaking of the sulfenamide bond.^{30,56} Compounds **12** and **13**, bearing an isothiazolinone and a benzisothiazolinone group, respectively, inhibited EGFR in a reversible manner, since inhibition was significantly reduced 8 h after removal from the medium (**12**, 80% and 25% inhibition at 1 and 8 h after treatment, respectively; **13**, 69% and 31%, respectively). Only the thiadiazole derivative **14** was able to produce a significant, yet partial, irreversible inhibition of EGFR, as demonstrated by 67% inhibition of autophosphorylation 8 h after treatment. This warhead has been employed to design active-site directed inhibitors of different enzymes with a cysteine in their active site.³⁰

The design of a covalent inhibitor presents the risk that enzyme inhibition is mainly the result of high warhead reactivity, which would result in nonspecific reactions with many possible off-targets. To test the role of the 4-anilinoquinazoline driving portion, which should be to confer target selectivity to poorly reactive warheads, we synthesized compounds **15** and **16** (Scheme 2 and Table 1), where two of the most active cysteine-trap portions of the series were linked to a simple naphthalene nucleus. In principle, the naphthalene ring is not able to recognize the molecular target because it lacks the structural elements required for interaction with the ATP-binding site of EGFR.⁵⁷ As expected, compound **15**, carrying an epoxysuccinic group analogue to compound **4**, and compound **16**, containing the same side chain as compound **7**, did not inhibit EGFR, demonstrating that target specificity of the series is due to driver-portion recognition within the EGFR active site. Interestingly, compounds **15** and **16** exhibited less than 10% inhibition of A431 cell proliferation at concentrations up to 10 μ M, indicating the absence of nonspecific cellular toxicity of the considered warheads (data not shown).

Table 2. Viability Inhibition of H1975 Gefitinib-Resistant Cell Line^a

compd	H1975 cell line, IC ₅₀ (μ M)
1	8.26 \pm 1.11
2	0.61 \pm 0.05
3	19.5 \pm 2.46
4	6.76 \pm 0.60
6	1.72 \pm 0.47
8	7.82 \pm 1.19
9	11.0 \pm 1.08

^aConcentration that inhibits by 50% the proliferation of NSCLC H1975. The cell proliferation was determined by the MTT assay after 72 h of incubation with compounds (0.1–20 μ M). Mean values of three independent experiments \pm SEM are reported.

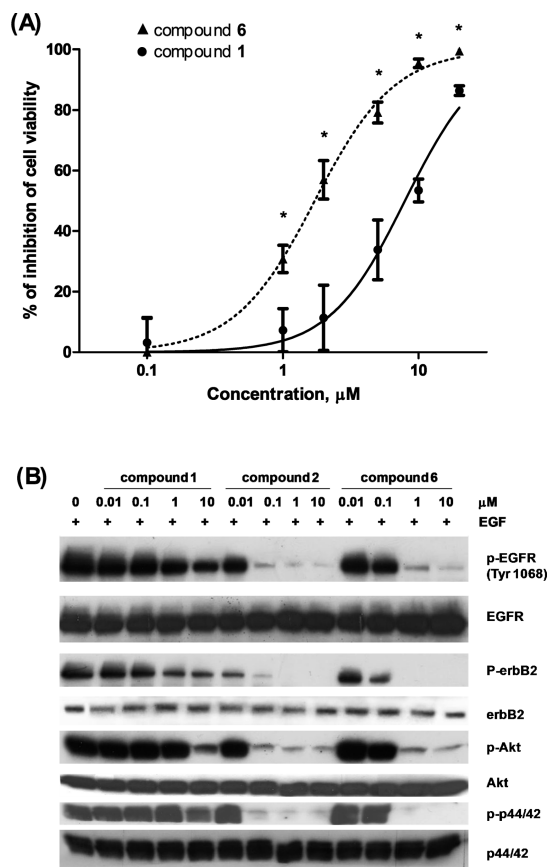


Figure 4. Effectiveness of irreversible EGFR inhibitor **6** in H1975 NSCLC cell line. (A) Antiproliferative effects of compound **6** (\blacktriangle) in comparison with **1** (\bullet) on H1975 cell line, harboring the resistance-associated mutation T790M. Cell proliferation was determined by MTT assay, as described in the Experimental Section. Results are reported as the mean \pm SD of three independent experiments: (*) $P < 0.01$ for each dose versus **1**; $n = 3$. (B) Comparison of compounds **6**, **1**, and **2** in their ability to suppress EGFR autophosphorylation (p-EGFR), erbB2 autophosphorylation (p-erbB2), and phosphorylation of downstream effectors AKT (p-Akt) and MAPK (p-p44/42) in H1975 cells. Total EGFR, erbB2, AKT, and MAPK are shown as loading controls.

Moreover, the formation of conjugates with glutathione was evaluated in aqueous buffered solution by LC–UV and LC–ESI–MS (see Experimental Section) to assess the intrinsic reactivity of the warheads toward a thiol derivative. Neither the epoxy derivatives **4** and **15** nor the phenoxyacetamides **7** and **16** gave any measurable adduct with GSH after 1 h of incubation (data not shown). On the other hand the acrylamide **2** showed conversion of $36.2 \pm 1.9\%$ of the starting

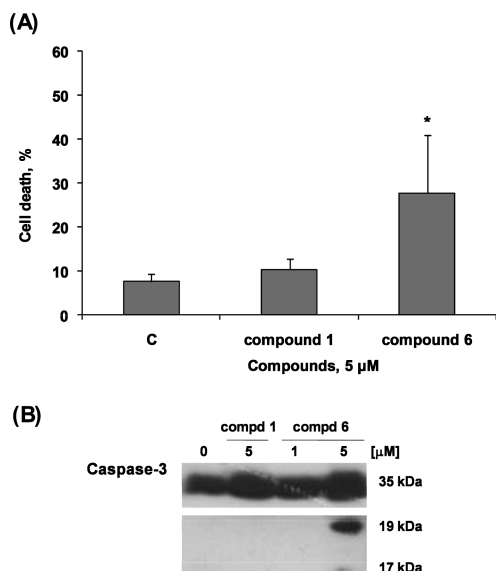


Figure 5. Effect of compound 6 on H1975 cell death. (A) H1975 cells were treated with the indicated concentration of compound 1 and compound 6 for 72 h and then analyzed with propidium iodide/Hoechst 33342 staining to assess cell death: (*) $P < 0.01$ for each dose versus control; $n = 3$. (B) At the same time the cleavage of procaspase-3 was assessed on lysate proteins by Western blotting. The migration position of each full-length procaspase and those of its processing products are indicated.

compound to its GSH conjugate ($[M + H]^+ = 676.11$) under the same conditions (mean \pm SD; $n = 3$).

We next tested the antiproliferative activity of compounds exhibiting highest potency as EGFR irreversible inhibitors on the gefitinib-resistant H1975 NSCLC cell line, by MTT assay. Results were compared with those of the reference compounds 1–3 in the same test. As reported in Table 2, compound 4 exhibited a dose-dependent inhibition of H1975 cell proliferation with an IC_{50} similar to that of 1 (IC_{50} s of 6.76 and 8.26 μ M, respectively). Interestingly, introduction of the basic piperidino group on the reactive side chain made compound 6 4 times more active than 1 on H1975 cells (Figure 4A and Table 2), with an antiproliferative IC_{50} of 1.72 μ M. The 6-phenoxyacetamide derivatives 8 and 9 showed IC_{50} on H1975 cells proliferation in the same range of the reference compound 1 (IC_{50} of 7.82 and 11.02 μ M, respectively).

We then examined the ability of compound 6 to inhibit EGFR signaling in the NSCLC cell line H1975 harboring the T790M mutation. 1 and 2 were used as reference compounds. Results of Western blot analysis are illustrated in Figure 4B. Compound 6 produced a dose-dependent inhibition of EGFR and erbB2 autophosphorylation with complete inhibition at 1 μ M. By contrast, 1 showed marginal activity on EGFR and erbB2 in H1975 cells up to 10 μ M. Compound 6 was also considerably more effective than 1 in inhibiting the two major signaling pathways activated by EGFR, the PI3K/AKT/mTOR and the RAS/RAF/MAPK cascades having a central role in controlling cell survival, cell growth, and proliferation (Figure 4B).

Finally, we observed that compound 6 killed more cells (25–30% at 5 μ M) when compared with control or cells treated with the reference compound 1 (Figure 5A) and was associated with caspase-3 activation (Figure 5B). After 2 days of treatment at 5 μ M, compound 6 significantly cleaved this proapoptotic protein from its inactive precursor form into

active fragments. These results suggest that this new irreversible inhibitor can have both a cytostatic and a cytotoxic effect on the H1975 cancer cell line. On the other hand, compound 6 proved to have only a weak cytotoxic profile on a cell line where proliferation is not driven by EGFR activity, excluding off-target general cytotoxic effects. In fact, compound 6 at 10 μ M inhibited less than 50% of SW620 cell proliferation, similar to what was observed for 1 and for the epoxysuccinic derivative 4, while the acrylamide derivative 2 gave an IC_{50} of $8.23 \pm 1.08 \mu$ M (Table S3, Supporting Information).

Conclusion

We report here an exploration of possible warheads for EGFR inhibition, extended to the most important classes of clinically exploitable ones. We investigated warheads that covalently react with cysteine via nucleophilic addition (epoxides 4–6), nucleophilic substitution (phenoxyacetamides 7–9), carbamylation (carbamate 10), Pinner reaction (nitrile 11), and disulfide bond formation (isothiazolinone 12, benzisothiazolinone 13, thiadiazole 14).

Compounds from different chemical classes proved efficient in irreversibly inhibiting EGFR autophosphorylation.⁵⁸ Epoxy derivatives 4–6 showed potencies comparable to that of the acrylamide reference compound 2. As expected from the structure of EGFR, the introduction of a terminal basic group (compound 6) significantly improved inhibition of both EGFR autophosphorylation and cell proliferation, suggesting that the identified compounds could be starting points for further structure-based optimization. Compound 6 inhibited EGFR downstream signaling pathways and showed cytostatic and cytotoxic activities on gefitinib-resistant NSCLC cells (H1975). Another interesting warhead is represented by the phenoxyacetamides (7–9), which in principle can release a leaving group on nucleophilic substitution and may be considered for a multidrug approach in cancer treatment. Promising results were also observed with the carbamate 10 and the thiadiazole 14.

In conclusion, the results described here extend the chemical diversity of new irreversible EGFR inhibitors, and similar chemical approaches could be exploited to design compounds targeting noncatalytic cysteines by covalent bond formation.

Experimental Section

Reagents were obtained from commercial suppliers and used without further purification. Solvents were purified and stored according to standard procedures. Anhydrous reactions were conducted under a positive pressure of dry N_2 . Reactions were monitored by TLC, on Kieselgel 60 F 254 (DC-Alufolien, Merck). Final compounds and intermediates were purified by flash chromatography (SiO_2 60, 40–63 μ m). Microwave reactions were conducted using a CEM Discover synthesis unit (CEM Corp., Matthews, NC). Melting points were not corrected and were determined with a Gallenkamp melting point apparatus. The 1H NMR spectra were recorded on a Bruker 300 MHz Avance spectrometer. Chemical shifts (δ scale) are reported in parts per million (ppm) relative to the central peak of the solvent. 1H NMR spectra are reported in the following order: multiplicity, approximate coupling constant (J value) in hertz (Hz), and number of protons; signals were characterized as s (singlet), d (doublet), dd (doublet of doublets), t (triplet), dt (doublet of triplets), q (quartet), m (multiplet), br s (broad signal). Mass spectra were recorded using an API 150 EX instrument (Applied Biosystems/MDS SCIEX, Foster City, CA). Liquid chromatography/mass spectrometry analysis was performed on an Agilent 1100 LC gradient system and on an Applied Biosystem 150-EX

single quadrupole mass spectrometer equipped with a TurboIon-Spray ion source working in positive ion mode. Compounds **1**,⁵⁹ **2**,³⁴ and **3**³⁵ were synthesized according to literature methods. The final compounds were analyzed on ThermoQuest (Italia) FlashEA 1112 elemental analyzer for C, H, and N. Analyses were within $\pm 0.4\%$ of the theoretical values (Table S1, Supporting Information). All tested compounds were $>95\%$ pure by elemental analysis.

(2R,3S)-Ethyl 3-(Piperidin-1-ylmethyl)oxirane-2-carboxylate (34). A 0 °C cooled solution of (2R,3S)-ethyl 3-(hydroxymethyl)oxirane-2-carboxylate **33**³⁹ (405 mg, 2.77 mmol) and Et₃N (582 μ L, 4.16 mmol) in anhydrous CH₂Cl₂ (12 mL) was stirred for 30 min before the dropwise addition of methanesulfonyl chloride (MsCl) (407 μ L, 4.16 mmol). The mixture was then stirred for 10 min at 0 °C and for 2 h at room temperature. Then the solvent was evaporated. The resulting yellow paste was dissolved in anhydrous DMF (12 mL), and KI (23 mg, 0.14 mmol) was added. The yellow solution was cooled to 0 °C and stirred for 5 min before the dropwise addition of anhydrous piperidine (830 μ L, 8.31 mmol). The resulting suspension was slowly warmed to room temperature and stirred for 7 days, diluted with saturated aqueous NaHCO₃ (85 mL), and extracted with Et₂O. The combined organic layers were dried and evaporated to give a brown oil that was purified by silica gel chromatography (CH₂Cl₂/MeOH, 100:0 to 96:4), furnishing **34** as a yellow oil (30%): ¹H NMR (300 MHz, CDCl₃) δ 1.25 (t, J = 7.1 Hz, 3H), 1.39 (m, 2H), 1.55 (m, 4H), 2.31 (dd, J = 13.6, 6.4 Hz, 1H), 2.36–2.55 (m, 4H), 2.71 (dd, J = 13.6, 3.4 Hz, 1H), 3.19 (d, J = 2.0 Hz, 1H), 3.29 (m, 1H), 4.18 (m, 2H).

Potassium (2R,3S)-3-(Piperidin-1-ylmethyl)oxirane-2-carboxylate (19). To an ice cold stirring solution of (2R,3S)-ethyl 3-(piperidin-1-ylmethyl)oxirane-2-carboxylate **34** (170 mg, 0.80 mmol) in absolute EtOH (1 mL), a solution of KOH (45 mg, 0.8 mmol) in absolute EtOH (1.5 mL) was added dropwise. The resulting mixture was stirred for 2 h at 0 °C. The solvent was removed under reduced pressure, and the residue was washed with petroleum ether. The product **19** was obtained as a pale-brown solid (83%): mp >230 °C; MS (APCI) m/z 184.2; ¹H NMR (300 MHz, CDCl₃) δ 1.49 (m, 2H), 1.63 (m, 4H), 2.32 (dd, J = 13.4, 6.7 Hz, 1H), 2.54 (m, 4H), 2.74 (dd, J = 13.4, 3.7 Hz, 1H), 3.02 (d, J = 2.16 Hz, 1H), 3.12 (m, 1H).

2-(3-Oxoisothiazolin-2-yl)acetic acid (25). A suspension of ethyl 2-(3-oxoisothiazolin-2-yl)acetate **37**⁴² (200 mg, 1.07 mmol) in 1 M trifluoroacetic acid (TFA) (25 mL, 25 mmol) was refluxed for 12 h and then evaporated. The residue was dried at 50–55 °C in vacuo to yield **25** (98%) as a white solid: mp 171–172 °C; ¹H NMR (300 MHz, DMSO-*d*₆) δ 4.41 (s, 2H), 6.19 (d, J = 6.2 Hz, 1H), 8.51 (d, J = 6.2 Hz, 1H).

(2R,3R)-Ethyl 3-(4-(3-Bromoanilino)quinazolin-6-ylcarbamoyl)oxirane-2-carboxylate (4). **Method A**. Dichloromethylene dimethyliminium chloride (356 mg, 2.19 mmol) was added to a stirred solution of (2R,3R)-2,3-epoxysuccinic acid monoethyl ester **17**³⁸ (350 mg, 2.19 mmol) in anhydrous CH₂Cl₂ (10 mL). After the reactants were stirred for 1 h with ice-cooling, 6-amino-4-(3-bromoanilino)quinazoline **3** (458 mg, 1.46 mmol) and NaHCO₃ (613 mg, 7.3 mmol) were added, and the suspension was stirred for 1 h at 0 °C. The mixture was washed with water, dried, and concentrated to obtain the crude compound. Crystallization from MeOH gave the pure product **4** as white crystals (60%): mp (MeOH) >230 °C (dec); MS (APCI) m/z 458.3, 459.2; ¹H NMR (300 MHz, DMSO-*d*₆) δ 1.26 (t, J = 7.1 Hz, 3H), 3.82 (d, J = 1.7 Hz, 1H), 3.93 (d, J = 1.7 Hz, 1H), 4.23 (q, J = 7.1 Hz, 2H), 7.29 (d, J = 8.1 Hz, 1H), 7.35 (t, J = 7.9 Hz, 1H), 7.82–7.92 (m, 3H), 8.16 (br s, 1H), 8.60 (s, 1H), 8.72 (d, J = 1.3 Hz, 1H), 9.93 (br s, 1H), 10.80 (br s, 1H). Anal. (C₂₀H₁₇BrN₄O₄) C, H, N.

(2S,3S)-Ethyl 3-(4-(3-Bromoanilino)quinazolin-6-ylcarbamoyl)oxirane-2-carboxylate (5). 6-Amino-4-(3-bromoanilino)quinazoline **3** was reacted with (2S,3S)-2,3-epoxysuccinic acid monoethyl ester **18**⁴⁰ according to the procedure described in

Method A. The crude product was purified by silica gel chromatography (CH₂Cl₂/MeOH, 99:1 to 97:3) to give **5** (66%) as a white solid: mp (MeOH) >230 °C; MS (APCI) m/z 457.9, 459.3; ¹H NMR (300 MHz, DMSO-*d*₆) δ 1.26 (t, J = 7.2 Hz, 3H), 3.81 (d, J = 1.7 Hz, 1H), 3.92 (d, J = 1.7 Hz, 1H), 4.23 (q, J = 7.1 Hz, 2H), 7.29 (d, J = 8.1 Hz, 1H), 7.35 (t, J = 7.8 Hz, 1H), 7.80–7.87 (m, 2H), 7.89 (dd, J = 9.0, 2.2 Hz, 1H), 8.16 (s, 1H), 8.60 (s, 1H), 8.72 (s, 1H), 9.94 (br s, 1H), 10.80 (br s, 1H). Anal. (C₂₀H₁₇BrN₄O₄) C, H, N.

(2R,3S)-N-(4-(3-Bromoanilino)quinazolin-6-yl)-3-(piperidin-1-ylmethyl)oxirane-2-carboxamide (6). **Method B**. To a suspension of potassium (2R,3S)-3-(piperidin-1-ylmethyl)oxirane-2-carboxylate **19** (58 mg, 0.26 mmol) in anhydrous DMF (2 mL), *O*-(benzotriazol-1-yl)-*N,N,N',N'*-tetramethyluronium hexafluorophosphate (HBTU) (205 mg, 0.54 mmol) was added at room temperature. The mixture was stirred for 40 min before the dropwise addition of 6-amino-4-(3-bromoanilino)quinazoline **3** (80 mg, 0.26 mmol) in DMF (2 mL). The reaction mixture was stirred for 16 h, the solvent was removed, and the residue was dissolved in CH₂Cl₂ and washed with saturated aqueous Na₂CO₃. The organic phase was evaporated and the crude product purified by silica gel chromatography (CH₂Cl₂/MeOH, 99:1 to 97:3) to give **6** as a pale-yellow solid (30%): mp >230 °C; MS (APCI) m/z 482.2, 484.2; ¹H NMR (300 MHz, CD₃OD) δ 1.41–1.43 (m, 2H), 1.53–1.64 (m, 4H), 2.36 (dd, J = 13.6, 6.7 Hz, 1H), 2.48–2.56 (m, 4H), 2.80 (dd, J = 13.7, 3.4 Hz, 1H), 3.30–3.34 (m, 1H), 3.39 (d, J = 1.89 Hz, 1H), 7.21–7.22 (m, 2H), 7.64–7.69 (m, 2H), 7.77 (dd, J = 9.0, 2.2 Hz, 1H), 8.03 (s, 1H), 8.45 (s, 1H), 8.56 (d, J = 2.1 Hz, 1H). Anal. (C₂₃H₂₄BrN₅O₂) C, H, N.

N-(4-(3-Bromoanilino)quinazolin-6-yl)-2-phenoxyacetamide (7). **Method C**. Phenoxyacetic acid **20** (361 mg, 2.37 mmol) was added to a stirred suspension of PCl₅ (490 mg, 2.37 mmol) in CH₂Cl₂ (15 mL) at room temperature. The reactants were refluxed for 30 min and then cooled to room temperature, and 6-amino-4-(3-bromoanilino)quinazoline **3** (500 mg, 1.59 mmol) was added in 10 min. After refluxing for 2 h, the mixture was cooled in an ice/water bath, an amount of 2.5 mL of water was added, the mixture was stirred for 30 min, and then Na₂CO₃ was added. The solid was filtered and purified by silica gel chromatography (CH₂Cl₂/MeOH, 99:1 to 97:3) to afford **7** as a white solid (77%): mp (EtOH/water) 212 °C; MS (APCI) m/z 449.0, 451.0; ¹H NMR (300 MHz, DMSO-*d*₆) δ 4.79 (s, 2H), 6.99 (t, J = 7.4 Hz, 1H), 7.05 (d, J = 7.8 Hz, 2H), 7.27–7.36 (m, 4H), 7.80 (d, J = 8.9 Hz, 1H), 7.85 (d, J = 7.9 Hz, 1H), 7.95 (dd, J = 9.0, 2.1 Hz, 1H), 8.16 (s, 1H), 8.58 (s, 1H), 8.74 (d, J = 1.7 Hz, 1H), 9.93 (s, 1H), 10.44 (s, 1H). Anal. (C₂₂H₁₇BrN₄O₂) C, H, N.

N-(4-(3-Bromoanilino)quinazolin-6-yl)-2-(4-fluorophenoxy)acetamide (8). 6-Amino-4-(3-bromoanilino)quinazoline **3** was reacted with 2-(4-fluorophenoxy)acetic acid **21** according to the procedure described in Method C. The crude product was purified by silica gel chromatography (CH₂Cl₂/MeOH, 99:1 to 97:3) to give **8** (67%) as a white solid: mp (EtOH/water) 224 °C; MS (APCI) m/z 467.3, 469.1; ¹H NMR (300 MHz, DMSO-*d*₆) δ 4.78 (s, 2H), 7.07 (dd, J = 9.2, 4.3 Hz, 2H), 7.15–7.21 (m, 2H), 7.27–7.37 (m, 2H), 7.85 (m, 2H), 7.95 (dd, J = 8.2, 1.4 Hz, 1H), 8.16 (br s, 1H), 8.59 (s, 1H), 8.74 (br s, 1H), 9.93 (br s, 1H), 10.44 (br s, 1H). Anal. (C₂₂H₁₆BrFN₄O₂) C, H, N.

N-(4-(3-Bromoanilino)quinazolin-6-yl)-2-(perfluorophenoxy)acetamide (9). 6-Amino-4-(3-bromoanilino)quinazoline **3** was reacted with 2-(perfluorophenoxy)acetic acid **22** according to the procedure described in Method C. The crude product was purified by silica gel chromatography (CH₂Cl₂/MeOH, 99:1 to 97:3) to give **9** (50%) as a white solid: mp 220–221 °C; MS (APCI) m/z 539.1, 541.1; ¹H NMR (300 MHz, DMSO-*d*₆) δ 4.99 (s, 2H), 7.24–7.34 (m, 2H), 7.75–7.87 (m, 3H), 8.11 (s, 1H), 8.55 (s, 1H), 8.66 (s, 1H), 9.91 (br s, 1H), 10.50 (br s, 1H). Anal. (C₂₂H₁₂BrF₅N₄O₂) C, H, N.

N-(4-(3-Bromoanilino)quinazolin-6-yl)-2-cyanoacetamide (11). 6-Amino-4-(3-bromoanilino)quinazoline **3** was reacted with

2-cyanoacetic acid **24** according to the procedure described in Method C. The crude product was purified by silica gel chromatography (EtOAc) to give **11** (55%) as white solid: mp (EtOH/water) 263 °C; MS (APCI) m/z 382.0, 384.1; ^1H NMR (300 MHz, DMSO- d_6) δ 4.00 (s, 2H), 7.30–7.35 (m, 2H), 7.81–7.86 (m, 3H), 8.15 (t, J = 1.7 Hz, 1H), 8.59 (s, 1H), 8.70 (s, 1H), 9.95 (s, 1H), 10.64 (s, 1H). Anal. ($\text{C}_{17}\text{H}_{12}\text{BrN}_5\text{O} \cdot 1.5\text{H}_2\text{O}$) C, H, N.

N-[2-[(4-(3-Bromoanilino)quinazolin-6-yl)amino]-2-oxoethyl]Phenylcarbamate (**10**). Method D. 2-(Phenoxy-carbonylamino)-acetic acid **23** (375 mg, 1.92 mmol) and *N,N'*-dicyclohexylcarbodiimide (DCC) (416 mg, 1.04 mmol) were added to a solution of **3** (400 mg, 1.28 mmol) in anhydrous DMF (6 mL) at 0 °C. The mixture was stirred 16 h at room temperature, the solid was removed by filtration, and the filtrate was evaporated in vacuo to obtain the crude product, which was purified by silica gel chromatography (EtOAc). The pure product **10** (55%) appeared as a white solid: mp (EtOH/water) > 250 °C (dec); MS (APCI) m/z 492.1; ^1H NMR (300 MHz, DMSO- d_6) δ 4.20 (s, 2H), 6.73–6.78 (m, 3H), 7.15 (t, J = 8.6 Hz, 2H), 7.32 (dt, J = 8.1, 1.6 Hz, 1H), 7.37 (t, J = 7.9 Hz, 1H), 7.82–7.93 (m, 3H), 8.21 (s, 1H), 8.50 (s, 1H), 8.57 (d, J = 1.7 Hz, 1H), 8.70 (s, 1H), 9.32 (s, 1H), 9.98 (br s, 1H). Anal. ($\text{C}_{25}\text{H}_{20}\text{BrN}_3\text{O}_3 \cdot 0.5\text{H}_2\text{O}$) C, H, N.

N-(4-(3-Bromoanilino)quinazolin-6-yl)-2-(3-oxoisothiazolin-2-yl)acetamide (**12**). 6-Amino-4-(3-bromoanilino)quinazoline **3** was reacted with 2-(3-oxoisothiazolin-2-yl)acetic acid **25** according to the procedure described in Method D. The crude product was purified by silica gel chromatography (EtOAc/MeOH, 99:1 to 90:10) to give **12** (40%) as a white solid: mp (EtOH/water) > 230 °C; MS (APCI) m/z 456.1, 458.3; ^1H NMR (300 MHz, DMSO- d_6) δ 4.65 (s, 2H), 6.24 (d, J = 6.2 Hz, 1H), 7.28 (d, J = 8.0 Hz, 1H), 7.33 (t, J = 7.9 Hz, 1H), 7.79–7.85 (m, 3H), 8.10 (s, 1H), 8.55 (d, J = 6.2 Hz, 1H), 8.55 (s, 1H), 8.71 (s, 1H), 9.94 (br s, 1H), 10.69 (br s, 1H). Anal. ($\text{C}_{19}\text{H}_{14}\text{BrN}_5\text{O}_2\text{S} \cdot 1.5\text{H}_2\text{O}$) C, H, N.

N-(4-(3-Bromoanilino)quinazolin-6-yl)-2-(3-oxobenzod[*d*]isothiazolin-2-yl)acetamide (**13**). 6-Amino-4-(3-bromoanilino)quinazoline **3** was reacted with 2-(3-oxobenzod[*d*]isothiazolin-2-yl)acetic acid **26** according to the procedure described in Method D. The crude product was purified by silica gel chromatography (EtOAc/*n*-hexane, 99:1) to afford **13** (50%) as a white solid: mp (MeOH) 238 °C; MS (APCI) m/z 506.1, 508.1; ^1H NMR (300 MHz, DMSO- d_6) δ 4.75 (s, 2H), 7.25–7.31 (m, 2H), 7.43 (t, J = 7.5 Hz, 1H), 7.69 (t, J = 7.8 Hz, 1H), 7.76–7.83 (m, 3H), 7.88 (d, J = 7.9 Hz, 1H), 7.98 (d, J = 8.5 Hz, 1H), 8.09 (s, 1H), 8.54 (s, 1H), 8.72 (s, 1H), 9.89 (br s, 1H), 10.66 (br s, 1H). Anal. ($\text{C}_{23}\text{H}_{16}\text{BrN}_5\text{O}_2\text{S} \cdot 0.5\text{H}_2\text{O}$) C, H, N.

N-(4-(3-Bromoanilino)quinazolin-6-yl)-3-isopropyl-1,2,4-thiadiazole-5-carboxamide (**14**). Method E. Potassium *tert*-butoxide (84 mg, 0.75 mmol) was added to a premixed mixture of ethyl 3-isopropyl-1,2,4-thiadiazole-5-carboxylate **27**⁴⁴ (150 mg, 0.75 mmol) and 6-amino-4-(3-bromoanilino)quinazoline **3** (235 mg, 0.75 mmol) in anhydrous DMF (1 mL). The reaction mixture was microwaved (150 W) to 100 °C for 8 min. The solution was diluted with water and extracted with EtOAc. The organic phase was evaporated to obtain the crude compound, which was purified by silica gel chromatography ($\text{CH}_2\text{Cl}_2/\text{MeOH}$, 99:1 to 97:3) to give **14** (50%) as pale-yellow crystals: mp (CH_2Cl_2) 224 °C; MS (APCI) m/z 469.0, 471.0; ^1H NMR (300 MHz, DMSO- d_6) δ 1.47 (d, J = 6.9 Hz, 6H), 3.43 (m, 1H), 7.34 (dt, J = 8.2, 1.5 Hz, 1H), 7.40 (t, J = 8.0 Hz, 1H), 7.90 (d, J = 8.9 Hz, 1H), 7.93 (d, J = 7.9 Hz, 1H), 8.20–8.23 (m, 2H), 8.68 (s, 1H), 8.93 (d, J = 1.8 Hz, 1H), 10.01 (s, 1H), 11.33 (br s, 1H). Anal. ($\text{C}_{20}\text{H}_{17}\text{BrN}_6\text{O}_5 \cdot 0.5\text{H}_2\text{O}$) C, H, N.

(2*R*,3*R*)-Ethyl 3-(Naphthalen-2-ylcarbamoyl)oxirane-2-carboxylate (**15**). Compound **15** was synthesized by coupling the carboxylic acid **17** and 2-naphthylamine **31** following the procedure described in Method A. Purification by silica gel chromatography (*n*-hexane/EtOAc, 90:10 to 70:30) gave the pure

compound (70%) as a white solid: mp (EtOH/water) 118–119 °C; MS (APCI) m/z 283.3; ^1H NMR (300 MHz, CDCl_3) δ 1.32 (t, J = 7.1 Hz, 3H), 3.66 (d, J = 1.9 Hz, 1H), 3.85 (d, J = 2.0 Hz, 1H), 4.29 (m, 2H), 7.39–7.49 (m, 3H), 7.77–7.83 (m, 4H), 8.18 (d, J = 2.0 Hz, 1H). Anal. ($\text{C}_{16}\text{H}_{15}\text{NO}_4$) C, H, N.

N-(Naphthalen-2-yl)-2-phenoxyacetamide (**16**). Compound **16** was synthesized by coupling the carboxylic acid **20** and 2-naphthylamine **31** using the procedure described in Method C. Purification by silica gel chromatography (*n*-hexane/EtOAc, 70:30) gave the pure compound (80%) as a pale-yellow solid: mp (EtOH/water) 142–144 °C; MS (APCI) m/z 184.3; ^1H NMR (300 MHz, CDCl_3) δ 4.65 (s, 2H), 7.00–7.09 (m, 3H), 7.33–7.55 (m, 5H), 7.77–7.82 (m, 3H), 8.25 (d, J = 1.7 Hz, 1H), 8.43 (br s, 1H). Anal. ($\text{C}_{18}\text{H}_{15}\text{NO}_2$) C, H, N.

Reactivity with Reduced Glutathione. The reactivity of compounds **4**, **15**, **7**, and **16** with reduced glutathione (GSH) was evaluated in an aqueous buffered solution (phosphate buffered saline, PBS, pH 7.4), at 37 °C and compared to that of the acrylamide **2**. Briefly, 10 μL of the compound standard solution in DMSO (1 mM) was diluted with 890 μL of PBS, pH 7.4. Then an amount of 100 μL of a freshly prepared GSH solution in PBS (20 mM) was added. Conversion of the compounds and formation of conjugates at 37 °C and at different time points were measured by LC–UV and LC–ESI–MS. The LC column used was a Phenomenex Synergi Fusion (2.0 mm \times 100 mm, 4 μm), and the mobile phase was a gradient of 50–10% aqueous trifluoroacetic acid (0.05%) in methanol in 10 min at the flow rate of 250 $\mu\text{L}/\text{min}$.

Kinase Assay. Evaluation of the effects of compounds on the kinase activity of human EGFR was performed by measuring the phosphorylation of the substrate Ulight-CAGAGAIETD-KEYYTVKD (JAK1) using a human recombinant enzyme expressed in insect cells⁶⁰ and the LANCE detection method,⁶¹ employing the Cerep EGFR kinase assay.⁶² Briefly, the test compound, reference compound, or water (control) was mixed with the enzyme (0.0452 ng) in a buffer containing 40 mM Hepes/Tris (pH 7.4), 0.8 mM EGTA/Tris, 8 mM MgCl_2 , 1.6 mM DTT, 0.008% Tween-20, and 100 nM poly-D-lysine. Thereafter, the reaction was initiated by the addition of 100 nM substrate and 10 μM ATP, and the mixture was incubated for 15 min at room temperature. For control basal measurements, the enzyme was omitted from the reaction medium. Following incubation, the reaction was stopped by the addition of 13 mM EDTA. After 5 min, the antiphospho-PT66 antibody labeled with europium chelate was added. After 60 min, the fluorescence transfer was measured at excitation wavelength of 337 nm and emission wavelength of 620 nm using a microplate reader (Envision, Perkin-Elmer). The concentration of compound that inhibited receptor phosphorylation by 50% (IC_{50}) was calculated from inhibition curves.

Cell Culture. The human A431 epidermoid cancer cell line was cultured in D-MEM 4.5 g/L glucose. NSCLC cell line H1975 and SW620 cell line were cultured in RPMI. All media were supplemented with 2 mmol/L-glutamine, 10% FCS. A431 was from ATCC. H1975 was kindly provided by Dr. E. Giovannetti (Department of Medical Oncology, VU University Medical Center, Amsterdam, The Netherlands) and was maintained under standard cell culture conditions at 37 °C in a water-saturated atmosphere of 5% CO_2 in air.

Antibodies and Reagents. Media were from Euroclone, and FBS was purchased from Gibco-BRL (Grand Island, NY). Monoclonal anti-EGFR, polyclonal anti-phospho-EGFR (Tyr1068), monoclonal anti-erbB2, monoclonal anti-phospho-erbB2 (Tyr 1221/1222), polyclonal Akt, polyclonal anti-phospho-Akt (Ser473), monoclonal anti-p44/42 MAPK, monoclonal anti-phospho-p44/42 MAPK (Thr202/Tyr204), and polyclonal anticaspase-3 antibodies were from Cell Signaling Technology (Beverly, MA). Horseradish peroxidase-conjugated (HRP) secondary antibodies were from Pierce. The enhanced chemiluminescence system (ECL) was from Millipore (Millipore,

MA). Reagents for electrophoresis and blotting analysis were obtained from, respectively, BIO-RAD Laboratories and Millipore.

Western Blot Analysis. Procedures for protein extraction, solubilization, and protein analysis by 1D PAGE are described elsewhere.⁶³ 50–100 μ g proteins from lysates were resolved by 5–15% SDS–PAGE and transferred to PVDF membranes (Millipore). The membranes were then incubated with primary antibody, washed, and then incubated with HRP-antimouse or HRP-antirabbit antibodies. Immunoreactive bands were visualized using an enhanced chemiluminescence system.

Autophosphorylation Assay. Inhibition of EGFR autophosphorylation was determined as previously described using specific antiphosphotyrosine and antitotal EGFR antibodies by Western blot analysis.¹⁵

Cell Growth Inhibition. Cell viability was assessed after 3 days of treatment by tetrazolium dye [3-(4,5-dimethylthiazol-2-yl)-2,5-diphenyltetrazolium bromide (MTT), Sigma, Dorset, U.K.] assay as previously described.⁶³ Representative results of at least three independent experiments were used for evaluation of dose–response curves, calculated from experimental points using Graph Pad Prism5 software. The concentration that inhibits 50% (IC₅₀) (e.g., the point at which viability is 50%) was extrapolated from the dose–response curves. The compounds were renewed every 24 h.

Cell Death. Cell death was assessed by morphology on stained (Hoechst 33342, propidium iodide) or unstained cells using light, phase contrast, and fluorescence microscopy.⁵⁵ Activation of caspase-3 was evaluated by Western blotting procedure as previously described.⁵⁵

Statistical Analysis. Statistical significances of differences between data were estimated using the two-tailed Student's *t* test.

Computational Studies. Docking simulations were performed with Glide 5.0⁶⁴ employing the crystal structure of the EGFR kinase domain covalently bound to **2** (PDB code 2BJF).⁴⁵ Molecular models of compounds **4–14** were built using Maestro,⁶⁵ and their geometries were optimized by energy minimization using the OPLS2003 force field⁶⁶ in combination with GB/SA⁶⁷ model for implicit solvent representation (water) to an energy gradient of 0.01 kcal/(mol·Å). The EGFR crystal structure was submitted to the protein preparation procedure of Maestro, which includes addition of missing side chains and hydrogens, assignment of tautomeric state of histidines maximizing the number of hydrogen bonds, and geometric optimization of the whole system to a root-mean-square displacement (rmsd) value of 0.3 Å. Docking simulations were performed starting from minimum energy conformations of compounds **4–14** placed in an arbitrary position within a region centered on the covalent inhibitor **2**, using enclosing and bounding boxes of 20 and 14 Å on each side, respectively. van der Waals radii of the protein atoms were not scaled, while van der Waals radii of the ligand atoms with partial atomic charges lower than |0.15| were scaled by 0.8. Standard precision (SP) mode was applied, and the first 10 poses with the highest *G*-score values were collected for each docked compound. The resulting binding poses were reranked according to the rmsd of the 4-anilinoquinazoline heavy atoms, taking the crystallized compound **2** as a reference structure.

Acknowledgment. Grant support was from the following: Ministero della Salute (Programma Straordinario di Ricerca Oncologica 2006), Regione Emilia Romagna; AIRC (Associazione Italiana per la Ricerca sul Cancro); Associazione Marta Nurizzo, Brugherio MI; Associazione Chiara Tassoni, Parma; A.VO.PRO.RI.T., Parma; Associazione Davide Rodella, Montichiari BS; Lega Italiana per la Lotta contro i Tumori, Sezione di Parma; and CONAD, Bologna.

Supporting Information Available: Combustion analytical data; docking of compounds **2**, **4**, **5**, and **7–14** within the EGFR active site; SW620 cells viability inhibition. This material is available free of charge via the Internet at <http://pubs.acs.org>.

References

- (1) Yarden, Y.; Sliwkowski, M. X. Untangling the ErbB signalling network. *Nat. Rev. Mol. Cell Biol.* **2001**, *2*, 127–137.
- (2) Teman, S.; Kawaguchi, H.; El-Naggar, A. K.; Jelinek, J.; Tang, H.; Liu, D. D.; Lang, W.; Issa, J. P.; Lee, J. J.; Mao, L. Epidermal growth factor receptor copy number alterations correlate with poor clinical outcome in patients with head and neck squamous cancer. *J. Clin. Oncol.* **2007**, *25*, 2164–2170.
- (3) Barker, A. J.; Gibson, K. H.; Grundy, W.; Godfrey, A. A.; Barlow, J. J.; Healy, M. P.; Woodburn, J. R.; Ashton, S. E.; Curry, B. J.; Sarlett, L.; Henthorn, L.; Richards, L. Studies leading to the identification of ZD1839 (Iressa): an orally active, selective epidermal growth factor receptor tyrosine kinase inhibitor targeted to the treatment of cancer. *Bioorg. Med. Chem. Lett.* **2001**, *11*, 1911–1914.
- (4) Moyer, J. D.; Barbacci, E. G.; Iwata, K. K.; Arnold, L.; Boman, B.; Cunningham, A.; Di Orto, C.; Doty, J.; Morin, M. J.; Moyer, M. P.; Neveu, M.; Pollack, V. A.; Pustilnick, L. R.; Reynolds, M. M.; Sloan, D.; Theleman, A.; Miller, P. Induction of apoptosis and cell cycle arrest by CP-358,774, an inhibitor of epidermal growth factor receptor tyrosine kinase. *Cancer Res.* **1997**, *57*, 4838–4848.
- (5) Lynch, T. J.; Bell, D. W.; Sordella, R.; Gurubhagavatula, S.; Okimoto, R. A.; Brannigan, B. W.; Harris, P. L.; Haserlat, S. M.; Supko, J. G.; Haluska, F. G.; Louis, D. N.; Christiani, D. C.; Settleman, J.; Haber, D. A. Activating mutations in the epidermal growth factor receptor underlying responsiveness of non-small-cell lung cancer to gefitinib. *N. Engl. J. Med.* **2004**, *350*, 2129–2139.
- (6) Kobayashi, S.; Boggon, T. J.; Dayaram, T.; Janne, P. A.; Kocher, O.; Meyerson, M.; Johnson, B. E.; Eck, M. J.; Tenen, D. G.; Halmos, B. EGFR mutation and resistance of non-small-cell lung cancer to gefitinib. *N. Engl. J. Med.* **2005**, *352*, 786–792.
- (7) Pao, W.; Miller, V. A.; Politi, K. A.; Riely, G. J.; Somwar, R.; Zakowski, M. F.; Heelan, R. T.; Kris, M. G.; Varmus, H. E. KRAS mutations and primary resistance of lung adenocarcinomas to gefitinib or erlotinib. *PLoS Med.* **2005**, *2*, e17.
- (8) Engelman, J. A.; Janne, P. A. Mechanisms of acquired resistance to epidermal growth factor receptor tyrosine kinase inhibitors in non-small cell lung cancer. *Clin. Cancer Res.* **2008**, *14*, 2895–2899.
- (9) Yun, C.-H.; Mengwasser, K. E.; Toms, A. V.; Woo, M. S.; Greulich, H.; Wong, K.-K.; Meyerson, M.; Eck, M. J. The T790M mutation in EGFR kinase causes drug resistance by increasing the affinity for ATP. *Proc. Natl. Acad. Sci. U.S.A.* **2008**, *105*, 2070–2075.
- (10) Camp, E. R.; Summy, J.; Bauer, T. V.; Liu, W.; Gallick, G. E.; Ellis, L. M. Molecular mechanisms of resistance to therapies targeting the epidermal growth factor receptor. *Clin. Cancer Res.* **2005**, *11*, 397–405.
- (11) Engelman, J. F.; Settleman, J. Acquired resistance to tyrosine kinase inhibitors during cancer therapy. *Curr. Opin. Gene Dev.* **2008**, *18*, 73–79.
- (12) Mukherji, D.; Spicer, J. Second-generation epidermal growth factor tyrosine kinase inhibitors in non-small cell lung cancer. *Expert Opin. Invest. Drugs* **2009**, *18*, 293–301.
- (13) Bikker, J. A.; Brooijmans, N.; Wissner, A.; Mansour, T. S. Kinase domain mutations in cancer: implications for small molecule drug design strategies. *J. Med. Chem.* **2009**, *52*, 1493–509.
- (14) Zhang, J.; Yang, P. L.; Gray, N. S. Targeting cancer with small molecule kinase inhibitors. *Nat. Rev. Cancer* **2009**, *9*, 28–39.
- (15) Fry, D. W.; Bridges, A. J.; Denny, W. A.; Doherty, A.; Greis, K. D.; Hicks, J. L.; Hook, K. E.; Keller, P. R.; Leopold, W. R.; Loo, J. A.; McNamara, D. J.; Nelson, J. M.; Sherwood, V.; Smail, J. B.; Trumpp-Kallmeyer, S.; Dobrusin, E. M. Specific, irreversible inactivation of the epidermal growth factor receptor and erbB2, by a new class of tyrosine kinase inhibitor. *Proc. Natl. Acad. Sci. U.S.A.* **1998**, *95*, 12022–12027.
- (16) Kwak, E. L.; Sordella, R.; Bell, D. W.; Godin-Heymann, N.; Okimoto, R. A.; Brannigan, B. W.; Harria, P. L.; Driscoli, D. R.; Fidias, P.; Lynch, T. J.; Rabindran, S. K.; McGinnis, J. P.; Sharma, S. V.; Isselbacher, K. J.; Settleman, J.; Haber, D. A. Irreversible inhibitors of the EGF receptor may circumvent acquired resistance to gefitinib. *Proc. Natl. Acad. Sci. U.S.A.* **2005**, *102*, 7665–7670.
- (17) Carter, T. A.; Wodicka, L. M.; Shah, N. P.; Velasco, A. M.; Fabian, M. A.; Treiber, D. K.; Milanov, Z. V.; Atteridge, C. E.; Biggs, V. H.; Edeen, P. T.; Floyd, M.; Ford, J. M.; Grotzfeld, R. M.; Herrgard, S.; Insko, D. E.; Mehta, S. A.; Patel, H. K.; Pao, W.;

- Sawyers, C. L.; Varmus, H.; Zarrinkar, P. P.; Lockhart, D. J. Inhibition of drug-resistant mutants of ABL, KIT, and EGF receptor kinases. *Proc. Natl. Acad. Sci. U.S.A.* **2005**, *102*, 11011–11016.
- (18) Godin-Heymann, N.; Ulkus, L.; Brannigan, B. W.; McDermott, U.; Lamb, J.; Maheswaran, S.; Settleman, J.; Haber, D. A. The T790M “gatekeeper” mutation in EGFR mediates resistance to low concentration of an irreversible EGFR inhibitor. *Mol. Cancer Ther.* **2008**, *7*, 874–879.
- (19) Slichenmyer, W. J.; Elliott, W. L.; Fry, D. W. CI-1033, a pan-erbB tyrosine kinase inhibitor. *Semin. Oncol.* **2001**, *28*, 80–85.
- (20) Rabindran, S. K.; Discifani, C. M.; Rosfjord, E. C.; Baxter, M.; Floyd, M. B.; Golas, J.; Hallett, W. A.; Johnson, B. D.; Nilakantan, D.; Overbeek, E.; Reich, M. F.; Shen, R.; Shi, X.; Tsou, H.-R.; Wang, Y.-F.; Wissner, A. Antitumor activity of HKI-272, an orally active, irreversible inhibitor of the Her-2 tyrosine kinase. *Cancer Res.* **2004**, *64*, 3958–3965.
- (21) Gill, A. L.; Verdonk, M.; Boyle, R. G.; Taylor, R. A comparison of physicochemical property profiles of marketed oral drugs and orally bioavailable anti-cancer protein kinase inhibitors in clinical development. *Curr. Top. Med. Chem.* **2007**, *7*, 1408–1422.
- (22) Tsou, H.-R.; Mamuya, N.; Johnson, B. D.; Reich, M. F.; Gruber, B. C.; Ye, F.; Nilakantan, R.; Shen, R.; Discifani, C.; DeBlanc, R.; Davis, R.; Koehn, F. E.; Greenberger, L. M.; Wang, Y.-F.; Wissner, A. 6-Substituted-4-(3-bromophenylamino)quinazolines as putative irreversible inhibitors of the epidermal growth factor receptor (EGFR) and human epidermal growth factor receptor (HER-2) tyrosine kinases with enhanced antitumor activity. *J. Med. Chem.* **2001**, *44*, 2719–2734.
- (23) Smaill, J. B.; Showalter, H. D. H.; Zhou, H.; Bridges, A. J.; McNamara, D. J.; Fry, D. W.; Nelson, J. M.; Sherwood, V.; Vincent, P. W.; Roberts, B. J.; Elliott, W. L.; Denny, W. A. Tyrosine kinase inhibitors. 18. 6-Substituted 4-anilinoquinazolines and 4-anilino-3,4-dihydropyrimidines as soluble, irreversible inhibitors of the epidermal growth factor receptor. *J. Med. Chem.* **2001**, *44*, 429–440.
- (24) Mishani, E.; Abourbeh, G.; Jacobson, O.; Dissoki, S.; Daniel, R. B.; Rozen, G.; Shaul, M.; Levitzki, A. High-affinity epidermal growth factor receptor (EGFR) irreversible inhibitors with diminished chemical reactivities as positron emission tomography (PET)-imaging agent candidates of EGFR overexpressing tumors. *J. Med. Chem.* **2005**, *48*, 5337–5348.
- (25) Antonello, A.; Tarozzi, A.; Morroni, F.; Cavalli, A.; Rosini, M.; Hrelia, P.; Bolognesi, M. L.; Melchiorre, C. Multitarget-directed drug design strategy: a novel molecule designed to block epidermal growth factor receptor (EGFR) and to exert proapoptotic effects. *J. Med. Chem.* **2006**, *49*, 6642–6645.
- (26) Wissner, A.; Tsou, H.-R.; Jonson, B. D.; Hamann, P. R.; Zhang, N. Substituted Quinazoline Derivatives and Their Use as Tyrosine Kinase Inhibitors. PCT Int. Appl. WO99/09016, **1999**.
- (27) Ban, S. H.; Usui, T.; Nabeyama, W.; Morita, H.; Fukuzawa, K.; Nakamura, H. Discovery of boron-conjugated 4-anilinoquinazoline as a prolonged inhibitor of EGFR tyrosine kinase. *Org. Biomol. Chem.* **2009**, *7*, 4415–4427.
- (28) Potashman, M. H.; Duggan, M. E. Covalent modifiers: an orthogonal approach to drug design. *J. Med. Chem.* **2009**, *52*, 1231–1246.
- (29) Powers, J. C.; Asgian, J. L.; Dogan Ekici, O.; Ellis James, K. Irreversible inhibitors of serine, cysteine, and threonine proteases. *Chem. Rev.* **2002**, *102*, 4639–4750.
- (30) Leung-Toung, R.; Zhao, Y.; Li, W.; Tam, T. F.; Karimian, K.; Spino, M. Thiol proteases: inhibitors and potential therapeutic targets. *Curr. Med. Chem.* **2006**, *13*, 547–581.
- (31) Overall, C. M.; Kleinfeld, O. Towards third generation matrix metalloproteinase inhibitors for cancer therapy. *Br. J. Cancer* **2006**, *94*, 941–946.
- (32) Arnold, L. A.; Kosinski, A.; Estebanez-Perpina, E.; Fletterick, R. J.; Guy, R. K. Inhibitors of the interaction of a thyroid hormone receptor and coactivators: preliminary structure–reactivity relationships. *J. Med. Chem.* **2007**, *50*, 5269–5280.
- (33) Mor, M.; Lodola, A.; Rivara, S.; Vacondio, F.; Duranti, A.; Tontini, A.; Sanchini, S.; Piersanti, G.; Clapper, J. R.; King, A. R.; Tarzia, G.; Piomelli, D. Synthesis and structure–reactivity relationship of fatty acid amide hydrolase inhibitors: modulation at the N-portion of biphenyl-3-yl alkylcarbamates. *J. Med. Chem.* **2008**, *51*, 3484–3498.
- (34) Smaill, J. B.; Palmer, B. D.; Rewcastle, G. W.; Denny, V. A.; McNamara, D. J.; Dobrusin, E. M.; Bridges, A. J.; Zhou, H.; Showalter, H. D. H.; Winters, R. T.; Leopold, V. R.; Fry, D. W.; Nelson, J. M.; Slintak, V.; Elliot, V. L.; Roberts, B. J.; Vincent, P. W.; Patmore, S. J. Tyrosine kinase inhibitors. 15. 4-(Phenylamino)quinazoline and 4-(phenylamino)pyrido[*d*]pyrimidine acrylamides as irreversible inhibitors of the ATP binding site of the epidermal growth factor receptor. *J. Med. Chem.* **1999**, *42*, 1803–1815.
- (35) Rewcastle, G. W.; Denny, W. A.; Bridges, A. J.; Zhou, H.; Cody, D. R.; McMichael, A.; Fry, D. W. Tyrosine kinase inhibitors: synthesis and structure–activity relationships for 4-[(phenylmethyl)amino]- and 4-[(phenylamino)quinazolines as potent adenosine 5'-triphosphate binding site inhibitors of the tyrosine kinase domain of the epidermal growth factor receptor. *J. Med. Chem.* **1995**, *38*, 3482–3487.
- (36) Roth, G. A.; Tai, J. J. A new synthesis of aryl substituted quinazolin-4(1*H*)-ones. *J. Heterocycl. Chem.* **1996**, *33*, 2051–2053.
- (37) Saito, S.; Komada, K.; Morowake, T. Diethyl (2*S*,3*R*)-2-(*N*-tert-butoxycarbonyl)amino-3-hydroxysuccinate. *Org. Synth.* **1995**, *73*, 184–200.
- (38) Korn, A.; Rudolph-Böhner, S.; Moroder, L. A convenient synthesis of optically pure (2*R*,3*R*)-2,3-epoxysuccinyl-dipeptides. *Tetrahedron* **1994**, *50*, 8381–8392.
- (39) Hayashi, Y.; Shoji, M.; Mukaiyama, T.; Gotoh, H.; Yamaguchi, S.; Nakata, M.; Kakeya, H.; Osada, H. First asymmetric total synthesis of synerazol, an antifungal antibiotic, and determination of its absolute stereochemistry. *J. Org. Chem.* **2005**, *70*, 5643–5654.
- (40) Tamai, M.; Yokoo, C.; Murata, M.; Oguma, K.; Sota, K.; Sato, E.; Kanaoka, Y. Efficient synthetic method for ethyl (+)-(2*S*,3*S*)-3-[(*S*)-3-methyl-1-(3-methylbutylcarbamoyl)butylcarbamoyl]-2-oxiranecarboxylate (EST), a new inhibitor of cysteine proteinase. *Chem. Pharm. Bull.* **1987**, *35*, 1098–1104.
- (41) Clerici, F.; Contini, A.; Gelmi, M. L.; Pocar, D. Isothiazoles. Part 14: 3-Aminosubstituted isothiazole dioxides and their mono- and dihalogeno derivatives. *Tetrahedron* **2003**, *59*, 9399–9408.
- (42) Lewis, S. N.; Miller, G. A.; Hausman, M.; Szamborski, E. C. 4-Isothiazolin-3-ones. A general synthesis from 3,3'-dithiodipropionamides. *J. Heterocycl. Chem.* **1971**, *8*, 571–580.
- (43) Bordini, F.; Catellani, P. L.; Morini, G.; Plazzi, P. V.; Silva, C.; Barocelli, E.; Chiavarini, M. 4-(3-Oxo-1,2-benzisothiazolin-2-yl)alkanoic, -phenylalkanoic, and -phenoxyalkanoic acids: synthesis and anti-inflammatory, analgesic and antipyretic properties. *Farmaco* **1989**, *44*, 795–807.
- (44) Buck, W. Herbicidal[1,2,4]thiadiazoles. U.S. Patent 5,583,092, **1996**.
- (45) Blair, J. A.; Rauh, D.; Kung, C.; Yun, C.-H.; Fan, Q.-W.; Rode, H.; Zhang, C.; Eck, M. J.; Weiss, W. A.; Shokat, K. M. Structure guided development of affinity probes for tyrosine kinases using chemical genetics. *Nat. Chem. Biol.* **2007**, *3*, 229–238.
- (46) Stamos, J.; Sliwowski, M. X.; Eigenbrot, C. Structure of the epidermal growth factor receptor kinase domain alone and in complex with a 4-anilinoquinazoline inhibitor. *J. Biol. Chem.* **2002**, *277*, 46265–46272.
- (47) Domarkas, J.; Dudouit, F.; Williams, C.; Qiyu, Q.; Banerjee, R.; Brahimi, F.; Jean-Claude, B. J. The Combi-targeting concept: synthesis of stable nitrosoureas designed to inhibit the epidermal growth factor receptor (EGFR). *J. Med. Chem.* **2006**, *49*, 3544–3552.
- (48) Tsou, H.-R.; Overbeek-Klumpers, E. G.; Hallett, W. A.; Reich, M. F.; Floyd, M. B.; Johnson, B. D.; Michalak, R. S.; Nilakantan, R.; Discifani, C.; Golas, J.; Rabindran, S. K.; Shen, R.; Shi, X.; Wang, Y.-F.; Upeslaci, J.; Wissner, A. Optimization of 6,7-disubstituted-4-(arylamino)quinoline-3-carbonitriles as orally active, irreversible inhibitors of human epidermal growth factor receptor-2 kinase activity. *J. Med. Chem.* **2005**, *48*, 1107–1131.
- (49) Fry, D. W. Mechanism of action of erb tyrosine kinase inhibitors. *Exp. Cell Res.* **2003**, *284*, 131–139.
- (50) Wissner, A.; Overbeek, E.; Reich, M. F.; Floyd, M. B.; Johnson, B. D.; Mamuya, N.; Rosfjord, E. C.; Discifani, C.; Davis, R.; Shi, X.; Rabindran, S. K.; Gruber, B. C.; Ye, F.; Hallett, W. A.; Nilakantan, R.; Shen, R.; Wang, Y.-F.; Greenberger, L. M.; Tsou, H.-R. Synthesis and structure–activity relationships of 6,7-disubstituted 4-anilinoquinazoline-3-carbonitriles. The design of an orally active, irreversible inhibitor of the tyrosine kinase activity of the epidermal growth factor receptor (EGFR) and the human epidermal growth factor receptor-2 (HER-2). *J. Med. Chem.* **2003**, *46*, 49–63.
- (51) Johnson, L. N. Protein kinase inhibitors: contributions from structure to clinical compounds. *Q. Rev. Biophys.* **2009**, *19*, 1–40.
- (52) Rachid, Z.; Brahimi, F.; Qiu, Q.; Williams, C.; Hartley, J. M.; Hartley, J. A.; Jean-Claude, B. J. Novel nitrogen mustard-armed combi-molecules for the selective targeting of epidermal growth factor receptor overexpressing solid tumors: discovery of an unusual structure–activity relationship. *J. Med. Chem.* **2007**, *50*, 2605–2608.
- (53) Smaill, J. B.; Rewcastle, J. W.; Loo, J. A.; Greis, K. D.; Chan, O. H.; Reyner, E. L.; Lipka, E.; Showalter, H. D. H.; Vincent, P. W.; Elliott, W. L.; Denny, W. A. Tyrosine kinase inhibitors. 17.

- Irreversible inhibitors of the epidermal growth factor receptor: 4-(phenylamino)quinazoline- and 4-(phenylamino)pyrido[3,2-*d*]-pyrimidine-6-acrylamides bearing additional solubilizing functions. *J. Med. Chem.* **2000**, *43*, 1380–1397.
- (54) Matheson, S. L.; McNamee, J.; Jean-Claude, B. J. Design of a chimeric 3-methyl-1,2,3-triazene with mixed receptor tyrosine kinase and DNA damaging properties: a novel tumour targeting strategy. *J. Pharmacol. Exp. Ther.* **2001**, *296*, 832–840.
- (55) Cavazzoni, A.; Alfieri, R.; Carmi, C.; Zuliani, V.; Galetti, M.; Fumarola, C.; Frazzi, R.; Bonelli, M.; Bordi, F.; Lodola, A.; Mor, M.; Petronini, P. G. Dual mechanism of action of the 5-benzylidene-hydantoin UPR1204 on lung cancer cell lines. *Mol. Cancer Ther.* **2008**, *7*, 361–370.
- (56) Alvarez-Sanchez, R.; Basketter, D.; Pease, C.; Lepoittevin, J.-P. Studies of chemical selectivity of hapten, reactivity, and skin sensitization potency. 3. Synthesis and studies on the reactivity toward model nucleophiles of the ¹³C-labeled skin sensitizers, 5-chloro-2-methylisothiazol-3-one (MCI) and 2-methylisothiazol-3-one (MI). *Chem. Res. Toxicol.* **2003**, *16*, 627–636.
- (57) Palmer, B. D.; Trumpp-Kallmeyer, S.; Fry, D. W.; Nelson, J. M.; Showalter, H. D. H.; Denny, W. A. Tyrosine kinase inhibitors. 11. Soluble analogues of pyrrolo- and pyrazoloquinazolines as epidermal growth factor receptor inhibitors: synthesis, biological evaluation, and modeling of the mode of binding. *J. Med. Chem.* **1997**, *40*, 1519–1529.
- (58) Mor, M.; Bordi, F.; Carmi, C.; Vezzosi, S.; Lodola, A.; Petronini, P. G.; Alfieri, R.; Cavazzoni, A. Composti Inibitori Irreversibili di EGFR con Attività Antiproliferativa. Italian Patent Application MI2008A002336, **2008**.
- (59) Gilday, J. P.; David, M. Process for the Preparation of 4-(3'-Chloro-4'-fluoroanilino)-7-methoxy-6-(3-morpholinopropoxy)quinazoline. PCT Int. Appl. WO2004/024703, **2004**.
- (60) Weber, W.; Bertics, P. J.; Gill, G. N. Immunoaffinity purification of the epidermal growth factor receptor. Stoichiometry of binding and kinetics of self-phosphorylation. *J. Biol. Chem.* **1984**, *259*, 14631–14636.
- (61) Olive, D. M. Quantitative methods for the analysis of protein phosphorylation in drug development. *Expert Rev. Proteomics* **2004**, *1*, 327–341.
- (62) www.cerep.fr.
- (63) Cavazzoni, A.; Petronini, P. G.; Galetti, M.; Roz, L.; Andriani, F.; Carbognani, P.; Rusca, M.; Fumarola, C.; Alfieri, R.; Sozzi, G. Dose-dependent effect of FHIT-inducible expression in Calu-1 lung cancer cell line. *Oncogene* **2004**, *23*, 8439–8446.
- (64) *Glide*, version 5.0; Schrödinger, LLC: New York, 2005.
- (65) *Maestro*, version 8.5; Schrödinger, LLC: New York, 2008.
- (66) Jorgensen, W. L.; Maxwell, D. S.; Tirado-Rives, J. Development and testing of the OPLS all-atom force field on conformational energetics and properties of organic liquids. *J. Am. Chem. Soc.* **1996**, *118*, 11225–11236.
- (67) Ghosh, A.; Sendrovic Rapp, C.; Friesner, R. A. Generalized Born model based on a surface integral formulation. *J. Phys. Chem. B* **1998**, *102*, 10983–10990.